

Soft Matter

Accepted Manuscript



This is an *Accepted Manuscript*, which has been through the Royal Society of Chemistry peer review process and has been accepted for publication.

Accepted Manuscripts are published online shortly after acceptance, before technical editing, formatting and proof reading. Using this free service, authors can make their results available to the community, in citable form, before we publish the edited article. We will replace this *Accepted Manuscript* with the edited and formatted *Advance Article* as soon as it is available.

You can find more information about *Accepted Manuscripts* in the [Information for Authors](#).

Please note that technical editing may introduce minor changes to the text and/or graphics, which may alter content. The journal's standard [Terms & Conditions](#) and the [Ethical guidelines](#) still apply. In no event shall the Royal Society of Chemistry be held responsible for any errors or omissions in this *Accepted Manuscript* or any consequences arising from the use of any information it contains.

COMMUNICATION

Influence of Sorbitol on Protein Crowding in Solution and Freeze-concentrated Phases

Cite this: DOI: 10.1039/x0xx00000x

S. Khodadadi^{a*}, N. J. Clark^b, A. McAuley^c, V. Cristiglio^d, J. E. Curtis^e, E. Y. Shalaev^f and S. Krueger^{g*}

Received 00th January 2012,

Accepted 00th January 2012

DOI: 10.1039/x0xx00000x

www.rsc.org/

Small-angle neutron scattering was employed to study protein crowding under freezing conditions that mimic those used in pharmaceutical processing. The results demonstrate that, although there is an increase in heterogeneity as the temperature is reduced, sorbitol reduces protein crowding in both solution and freeze-concentrated phases, thus protecting the protein from forming oligomers or irreversible aggregates.

Proteins are widely used as therapeutics for numerous diseases and conditions. Protein stability during processing and storage without any chemical and physical degradation is of great interest for the development of commercial applications. Many proteins are stored as frozen or freeze-dried (lyophilized) materials to minimize chemical and physical degradation during their shelf life. The stability of proteins in these solid states, as well as in solution is influenced by temperature, pH, concentration, co-solutes and additives such as surfactants^{1,2}. During the freezing of protein solutions, a major fraction of water molecules form crystalline ice. The remaining water molecules and all of the other solutes, including the protein and other excipients, remain mainly in the amorphous phase³ and form a freeze-concentrated region with a mass fraction of water around 30 %⁴. Freezing often causes destabilization of the protein, which may result in unfolding and irreversible aggregation due to 1) an increase in protein concentration, 2) changes in protein-protein interactions, 3) changes in pH, 4) changes in buffer salt concentration or ionic strength, 5) a reduction of hydrophobic interactions due to dehydration of the protein, and 6) the formation of ice-solution interfaces^{5,6}.

Different formulations are developed to reduce these effects during processing and storage. For instance, changes in pH can be controlled during the freezing process by optimal choice of buffer or by decreasing the buffer concentration, whereas protein degradation at ice-water interfaces can be controlled by minimizing the surface area of ice crystals, increasing the protein concentration or by using surfactants⁷. It has been suggested that surfactants reduce the formation of insoluble aggregates at interfaces by direct binding to the proteins and/or by competing with the protein for adsorption on denaturing surfaces such as ice-solution interfaces^{8,9}.

Polyhydroxy compounds, including carbohydrates (sugars) and sugar-alcohols, are also well-known cryo- and lyo-protectors, which minimize destabilization of proteins and biological systems during the freeze-drying processes. Their extensive hydrogen bonding capacity and ability to form amorphous (glass) phases are believed to contribute to their protective properties. However, phase separation, crystallization of solute and ice formation all can contribute to the destabilization of proteins, even in the presence of polyhydroxy components¹⁰⁻¹⁶.

Preferential hydration has been proposed as a mechanism of protein stabilization in aqueous solutions containing carbohydrates^{17,18}. In this scenario, the solute (sugar molecule) is preferentially excluded from the surface of the protein resulting in an increase in the chemical potential of the protein, which favors its native structure of protein¹⁰. The same mechanism has also been invoked as one possible explanation of the stabilization of proteins during freezing^{19,20}. During the drying process, the solute is thought to continue to protect the protein either through the glassy immobilization mechanism²¹, where the viscosity is sufficiently high to prevent destabilization, or the water replacement hypothesis, where the solute replaces the hydrogen bonds of the water as it is removed¹⁹. These studies point out that the carbohydrate molecules must be in the same phase as the protein to act effectively as stabilizers.

Characterization of protein structure and interactions in solutions, freeze-concentrated solutions, and dried systems is essential to both designing stable biopharmaceutical products and understanding the mechanisms for lyo- and cryo-protection of biological systems. Small-angle neutron scattering (SANS) uses low-energy thermal neutrons to probe information on nm to μm length scales without degrading the sample, making it a well-suited technique to study the mesoscopic structure of proteins in a variety of phases. In particular, SANS can investigate the nature of protein crowding and phase separation in the presence and absence of polyhydroxy components, providing insight into the interactions between the protein and solute molecules during all stages of the freeze-drying process. In this work, SANS was used to investigate protein crowding in the solution and freeze-concentrated phases using model systems consisting of lysozyme, sorbitol and water.

To mimic protein crowding during freezing, high water content (HWC) and low water content (LWC) samples were prepared with the same protein to sorbitol weight ratio. In this case, “water” refers to D₂O, which was used to reduce the background scattering due to hydrogen atoms. The HWC consisted of a D₂O mass fraction of 80 %, a sorbitol mass fraction of 15 %, and a lysozyme mass fraction of 5 %, and the LWC consisted of a D₂O mass fraction of 30 %, a sorbitol mass fraction of 52.5 %, and a lysozyme mass fraction of 17.5 %. SANS measurements in the temperature range of 298 K to 100 K were performed on the 30 m SANS instruments at the National Institute of Standards and Technology (NIST), Center for Neutron Research (NCNR) in Gaithersburg, MD²². The cooling rate was 4 K per minute and the heating rate was 2.6 K per minute. Sub-ambient DSC measurements were performed at Amgen, Inc. in Thousand Oaks, CA in a similar temperature range using the same cooling and heating rates. Details of the sample preparation, SANS theory, SANS and DSC measurements, and data treatment are presented in the Supporting Information†.

SANS scattering intensity $I(q)$ vs q curves for both the HWC and LWC in the studied temperature range are shown in Figure 1. Here,

$$q = \frac{4\pi \sin \theta}{\lambda}$$

, where λ is the neutron wavelength and 2θ is the scattering angle. The measurements were made during both cooling and heating cycles to investigate the change in heterogeneity of the solutions, phase separation, protein interaction distance, hysteresis and possible irreversible changes in the scattering profiles. The data can be divided into two regions: the low- q scattering intensity (LQS), defined by the q -range 0.002 Å⁻¹ to 0.025 Å⁻¹, and the high- q scattering intensity (HQS), defined by the q -range 0.025 Å⁻¹ to 0.25 Å⁻¹. The LQS corresponds to length scales of 10 nm to > 1 μm and the HQS represents length scales from 1 nm to 10 nm.

In this work, heterogeneity of the system is ascribed to a change in the LQS or HQS that represent structural changes on their corresponding length scales. The LQS for both the HWC and LWC is observed to increase upon cooling from 298 K to 100 K, indicating an increase in large-scale heterogeneities in the 10 nm to > 1 μm size range due at least in part to newly formed ice-solution, air-solution and air-ice interfaces. The exception is the HWC at 213 K, in which the LQS is essentially the same as at 298 K. It was confirmed from DSC experiments (Supporting Information, Fig. S3†) that ice could form below 213 K in both the HWC and LWC. Thus, an increase in the LQS upon cooling to 213 K is expected. The lack of the increase in the scattering at 213K could be due to minimal formation of air bubbles in the initial stage of ice formation.

In the HQS region of both the HWC and LWC, an interaction peak is present at $q \approx 0.07$ Å⁻¹. The intensity of this peak tends to decrease upon cooling, while a second peak becomes visible at $q \approx 0.17$ Å⁻¹, indicating an increase in heterogeneities in the 1 nm to 10 nm size range, due at least in part a change the partitioning of protein and sorbitol. The changes observed upon cooling in both the LQS and HQS are reversible when the system is reheated to 298 K (Fig. S4†). However, some hysteresis in the shape of the SANS curves is observed at 170 K and 213 K. Data taken on the D22 SANS instrument at the Institut Laue-Langevin using different cooling and heating rates showed qualitative agreement to the NIST data (data not shown).

The SANS data were fit to the “broad peak” function using the IGOR program with SANS macro routines developed at the NCNR²³. This function describes the scattering intensity at low q with a power law term and the intensity at high q with a term that resembles a Lorentzian function, except that the exponent, m , is not restricted to a value of 2. The function is defined as

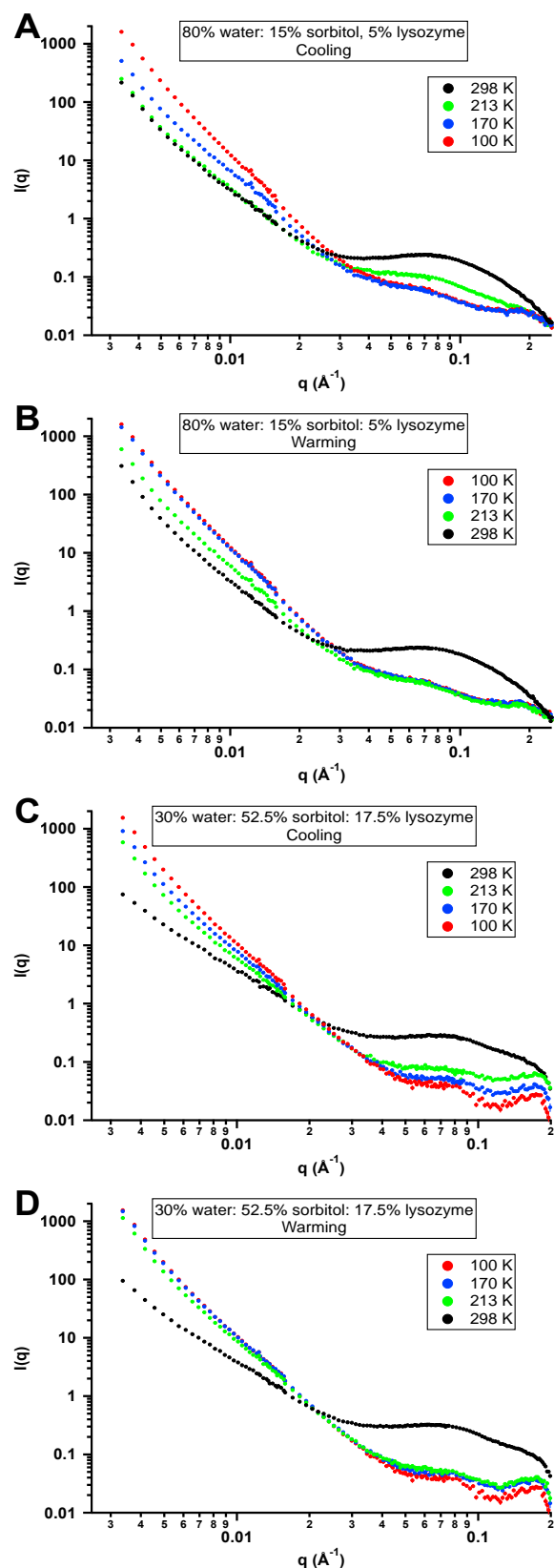


Figure 1. SANS $I(q)$ vs q curves during cooling from 298 K to 100 K for the A) HWC and C) LWC, and during heating from 298 K to 100 K for the B) HWC and D) LWC. The sharp cutoff of the data at $q \approx 0.2$ Å⁻¹ in C) and D) is a shadowing effect due to the sample holder geometry. Error bars represent standard deviations calculated from counting statistics.

$$I(q) = \frac{A}{q^n} + \frac{C}{1 + (q - q_0/\xi)^m} + B,$$
 where n is the power law exponent, found from the LQS, and q_0 is the position of the peak in the HQS. (See the Supporting Information† for further details.) The morphologies of the larger structures in the sample can be identified on the basis of n , where $n = 4$ indicates particles with a smooth surface, $3 < n < 4$ indicates particles with a rougher surface, and $2 < n < 3$ indicates a more network-like structure. Furthermore, the average center of mass distance, d , between the scattering particles can be found based on q_0 such that $d = 2\pi/q_0$. This is hereafter referred to as the d-spacing. The power law exponents and peak positions found for both the LWC and HWC are listed in Table S1†.

For both the LWC and HWC, the LQS decays with a power law exponent, n , that is between 3 and 4, indicative of rough interfaces. (The exception is the LWC at 298 K, which has $n < 3$ and is discussed below.) The values of n are closer to 3 at 298 K and increase to ≈ 4 as the temperature decreases to 100 K, accompanied by an increase in the LQS. The process is reversible as n returns to its original value upon warming back to 298 K (Fig. S4). This behavior is similar to that observed for 70 % sorbitol, 30 % D₂O solutions in the absence of protein²⁴, lysozyme solutions in the absence of sorbitol upon freezing^{25,26}, as well as for frozen D₂O solutions²⁶. This scattering is indicative of extensive heterogeneity on the length-scale of 10 nm to > 1000 nm that becomes more pronounced as the samples are cooled. Given the values of the power law exponent, the scattering was attributed to air bubbles that coalesce and increase in size in the glassy or frozen phases. Using SANS and contrast variation, it was verified that both the ice-air interfaces and large, loosely-associated lysozyme oligomers contribute to the LQS of frozen lysozyme samples^{25,26}. SANS and WANS results for 70 % sorbitol, 30 % D₂O solutions implied there is also increased long-range heterogeneity developed below the calorimetric glass transition temperature²⁴.

The LWC at 298 K has a power law exponent $n < 3$, implying a network-like structure (Supporting Information, Fig. S2†). MD simulations of solutions containing more than ≈ 50 % sugar²⁷ suggest the data might be explained by a space filling network of sorbitol. However, such a structure is less consistent with the increase in n with decreasing temperature. The higher values of n are more consistent with protein oligomers and/or micron-sized clusters of crowded protein molecules, such as those observed by dynamic light scattering for aqueous solutions of glucose, maltose and sucrose²⁸. Static and dynamic light scattering with nanoparticle tracking studies of solutions of low molar mass compounds also confirmed the existence of similar heterogeneities²⁹. Therefore, the LQS of the HWC and LWC contains contributions from large lysozyme-sorbitol clusters, lysozyme oligomers and possibly air-solution interfaces that increase upon cooling.

At 298 K, both the LWC and HWC have a main interaction peak at $q \approx 0.07 \text{ \AA}^{-1}$ in the HQS (Fig. 1). This peak is attributed to crowded lysozyme molecules with a d-spacing of approximately 90 Å. Even though the protein concentration in the LWC is more than three times that in the HWC, the interaction peak is observed to be in the same position in both cases. This behavior is not explained by a simple repulsive interaction between particles, where the peak position increases with increasing particle concentration (details in the Supporting Information†), as is observed for lysozyme solutions in absence of sorbitol²⁶. Rather, the HWC and LWC contain sorbitol-rich clusters of crowded lysozyme molecules that are the same distance apart, whereas the average concentration of solvent between clusters differs significantly. This fact alone indicates significant heterogeneity in the samples, even at room temperature.

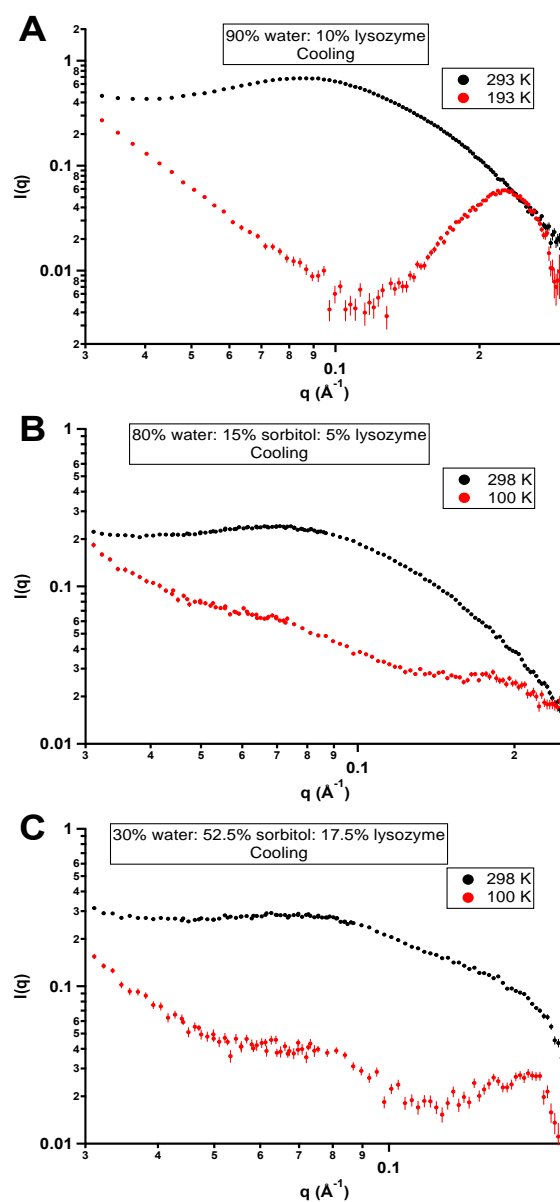


Figure 2. SANS $I(q)$ vs q curves for the A) lysozyme in the absence of sorbitol, B) the HWC sample and C) the LWC sample at room temperature and at the lowest measured temperatures. Error bars represent standard deviations calculated from counting statistics.

As the temperature is lowered, a decrease in the intensity of the main interaction peak and the appearance of a second interaction peak at $q \approx 0.17 \text{ \AA}^{-1}$, d-spacing $\approx 37 \text{ \AA}$, were observed for both the HWC and LWC (Fig. 1). The second interaction peak is attributed to an additional population of crowded lysozyme clusters, which is presumed to be lower in sorbitol content to allow closer packing of lysozyme molecules. The decrease in intensity of the main interaction peak occurs due to partitioning of lysozyme molecules into the second crowded population and/or into larger oligomers that contribute to the scattering in the LQS. The second interaction peak with d-spacing $\approx 37 \text{ \AA}$ is detectable even at 298 K for the LWC sample (Figs. 1C and 1D). This is perhaps not unexpected due to the much higher lysozyme concentration in the LWC.

The existence of a two populations of lysozyme clusters at 298 K for the LWC is consistent with a liquid-liquid phase separation

(LLPS). This is similar to the behavior seen for lysozyme solutions in a 0.4 M NaCl solution, where LLPS was observed above the freezing point for water²⁵. While no visible precipitate was observed in the LWC at temperatures between 277 K and 298 K, it is certainly possible that precipitates were present at 213 K and below in both the LWC and HWC, as SANS measures scattering particles whether they are in solution or suspension. However, the LLPS was observed by SANS in the LWC even in the absence of visible precipitation or phase separation.

A comparison of the HQS of lysozyme with and without sorbitol in the solution and freeze-concentrated phases is shown in Figure 2. For lysozyme in the absence of sorbitol, the d-spacing is ≈ 70 Å at 293 K (Fig. 2A) and that of the HWC and LWC are ≈ 90 Å at 298 K (Figs. 2B and 2C). The larger distance between molecules in the HWC and LWC due to the presence of sorbitol in the clusters implies reduced deleterious intermolecular associations, meaning that irreversible aggregation and oligomerization are less likely. This is especially important for the LWC, as the lysozyme concentration is 1.75 times higher than in the sample without sorbitol. Thus, the d-spacing would be less than 70 Å if sorbitol were not present to reduce the protein crowding.

The d-spacing of lysozyme in the absence of sorbitol changes dramatically upon freeze-concentration (Fig. 2A), to ≈ 30 Å at 193 K, suggesting that lysozyme is essentially close-packed in the freeze-concentrated phase²⁵. This observation is in contrast to the HWC and LWC (Figs. 2B and 2C), where the d-spacing of ≈ 90 Å persists down to 100 K even in the presence of the second population with d-spacing ≈ 37 Å. Thus, sorbitol reduces protein crowding in the second population compared to the sample without sorbitol. But, the most protection from deleterious intermolecular associations is afforded to the lysozyme molecules in the population with d-spacing of ≈ 90 Å, since this population persists in the freeze-concentrated phase.

Conclusions

In this work, for the first time, protein crowding of model systems was investigated under freezing conditions that typically used in pharmaceutical processing. SANS techniques were employed as a unique tool to detect protein crowding, phase separation and increase in large-scale heterogeneity in high water content (HWC) and low water content (LWC) samples that were prepared with the same protein to sorbitol weight ratio in the temperature range of 298 K to 100 K. The experiments revealed 1) changes in SANS scattering curves upon cooling that are completely reversible upon heating back to 298 K, 2) large-scale (10 nm to > 1 μ m) heterogeneities in both samples that increase upon cooling due to the formation of additional interfaces and contributions from large lysozyme and/or sorbitol structures, 2) heterogeneities on the 1 nm to 10 nm scale at 298 K, consisting of sorbitol-rich clusters of crowded proteins surrounded by areas of water containing little or no protein or sorbitol, 3) a second population of sorbitol-poor clusters of crowded proteins at 298 K in the LWC, with the average spacing between proteins about one-third less than the first population of clusters, 4) an identical sorbitol-poor population in the HWC that becomes visible at 213 K and below, and 5) that the sorbitol and protein do not phase separate in the freeze-concentrated state.

The results demonstrate that sorbitol reduces protein crowding in both the solution and freeze-concentrated phases, thus protecting the protein from forming oligomers or irreversible aggregates. However, further phase separation may occur during drying³⁰ such that the larger d-spacing population may not persist in the dry phase²⁶. Additional SANS studies of lysozyme-sorbitol samples after drying, storage and rehydration are expected to provide a better

understanding of protein-solute interactions during all stages of processing.

Acknowledgements

This work utilized facilities supported in part by the National Science Foundation under Agreement No. DMR-0944772. S. Khodadadi acknowledges funding from the National Research Council. We acknowledge M. Moore and M. Espinoza for help with the DSC measurements and T. Narayanan for useful discussions.

Notes and references

^aFaculty of Applied Sciences, Delft University of Technology, Delft, The Netherlands, Email: s.khodadadi@tudelft.nl.

^bCenter for Neutron Research, National Institute of Standards and Technology, Gaithersburg, MD, USA; Amgen Inc, Thousand Oaks, CA, USA, Email: nicholas.clark@nist.gov.

^cAmgen Inc, Thousand Oaks, CA, USA, Email: arnoldm@amgen.com

^dInstitut Laue-Langevin, Grenoble, France, Email: cristiglio@ill.fr.

^eCenter for Neutron Research, National Institute of Standards and Technology, Gaithersburg, MD, USA, Email: joseph.curtis@nist.gov.

^fAllergan, Inc., Irvine, CA, USA, Email: Shalaev_Evgenyi@allergan.com.

^gCenter for Neutron Research, National Institute of Standards and Technology, Gaithersburg, MD, USA, Email: susan.krueger@nist.gov.

* Corresponding authors

§ As used here, the term, “state”, refers to a form of matter, whereas the term, “phase” describes a region of space with uniform physical and/or chemical properties.

† Electronic Supporting Information (ESI) available: [Sample preparation; SANS and DSC experimental methods; SANS data treatment and theory; additional figures and table]. See DOI: 10.1039/c000000x/

1. E. Y. Chi, S. Krishnan, T. W. Randolph, and J. F. Carpenter, *Pharm. Res.*, 2003, **20**, 1325–1336.
2. T. Arakawa, Y. Kita, and J. F. Carpenter, *Pharm. Res.*, 1991, **8**, 285–291.
3. J. Dong, A. Hubel, J. C. Bischof, and A. Aksan, *J. Phys. Chem. B*, 2009, **113**, 10081–10087.
4. F. Franks, *Pure Appl. Chem.*, 1997, **69**, 915–920.
5. G. B. Strambini and M. Gonnelli, *Biophys. J.*, 2007, **92**, 2131–2138.
6. D. B. Varshney, J. A. Elliott, L. A. Gatlin, S. Kumar, R. Suryanarayanan, and E. Y. Shalaev, *J. Phys. Chem. B*, 2009, **113**, 6177–6182.
7. X. (Charlie) Tang and M. J. Pikal, *Pharm. Res.*, 2004, **21**, 191–200.
8. B. S. Chang, B. S. Kendrick, and J. F. Carpenter, *J. Pharm. Sci.*, 1996, **85**, 1325–1330.
9. L. Krielgaard, L. S. Jones, T. W. Randolph, S. Frokjaer, J. M. Flink, M. C. Manning, and J. F. Carpenter, *J. Pharm. Sci.*, 1998, **87**, 1593–1603.
10. T. W. Randolph, *J. Pharm. Sci.*, 1997, **86**, 1198–1203.
11. D. M. Piedmonte, C. Summers, A. McAuley, L. Karamujic, and G. Ratnaswamy, *Pharm. Res.*, 2006, **24**, 136–146.
12. M. C. Heller, J. F. Carpenter, and T. W. Randolph, *J. Pharm. Sci.*, 1996, **85**, 1358–1362.
13. K. Izutsu and S. Kojima, *Pharm. Res.*, 2000, **17**, 1316–1322.
14. K. A. Pikal-Cleland, N. Rodriguez-Hornedo, G. L. Amidon, and J. F. Carpenter, *Arch. Biochem. Biophys.*, 2000, **384**, 398–406.
15. B. S. Bhatnagar, M. J. Pikal, and R. H. Bogner, *J. Pharm. Sci.*, 2008, **97**, 798–814.
16. F. Franks, R. H. M. Hatley, and H. L. Friedman, *Biophys. Chem.*, 1988, **31**, 307–315.
17. J. C. Lee and S. N. Timasheff, *J. Biol. Chem.*, 1981, **256**, 7193–7201.
18. S. N. Timasheff, in *Protein-Solvent Interactions*, ed. R. B. Gregory, Marcel Dekker, New York, 1995, pp. 445–482.
19. J. F. Carpenter and J. H. Crowe, *Cryobiology*, 1988, **25**, 244–255.
20. J. F. Carpenter, J. H. Crowe, and T. Arakawa, *J. Dairy Sci.*, 1990, **73**, 3627–3636.

Journal Name

21. L. (Lucy) Chang, D. Shepherd, J. Sun, D. Ouellette, K. L. Grant, X. (Charlie) Tang, and M. J. Pikal, *J. Pharm. Sci.*, 2005, **94**, 1427–1444.
22. C. J. Glinka, J. G. Barker, B. Hammouda, S. Krueger, J. J. Moyer, and W. J. Orts, *J. Appl. Crystallogr.*, 1998, **31**, 430–445.
23. S. R. Kline, *J. Appl. Crystallogr.*, 2006, **39**, 895–900.
24. S. G. Chou, A. K. Soper, S. Khodadadi, J. E. Curtis, S. Krueger, M. T. Cicerone, A. N. Fitch, and E. Y. Shalaev, *J. Phys. Chem. B*, 2012, **116**, 4439–4447.
25. J. E. Curtis, A. McAuley, H. Nanda, and S. Krueger, *Faraday Discuss.*, 2012, **158**, 285–299.
26. J. E. Curtis, H. Nanda, S. Khodadadi, M. Cicerone, H. J. Lee, A. McAuley, and S. Krueger, *J. Phys. Chem. B*, 2012, **116**, 9653–9667.
27. A. Lerbret, P. Bordat, F. Affouard, M. Descamps, and F. Migliardo, *J. Phys. Chem. B*, 2005, **109**, 11046–11057.
28. D. L. Sidebottom and T. D. Tran, *Phys. Rev. E*, 2010, **82**.
29. M. Sedláč and D. Rak, *J. Phys. Chem. B*, 2013, **117**, 2495–2504.
30. V. Ragoonanan and A. Aksan, *Biophys. J.*, 2008, **94**, 2212–2227.

